

SUPPLEMENTAL MATERIAL**SUPPLEMENTAL METHOD****Reagents**

Sources of antibodies are as follows: anti-KLF2 (Santa Cruz Biotechnology, SC-18690), anti-KLF4 (R&D Systems, AF3640), anti-p57 (Santa Cruz Biotechnology, SC-56341), anti-FGFR3 (Santa Cruz Biotechnology, SC-123), anti-Prox1 (rabbit polyclonal antibody generated by the authors), anti- β -actin (Sigma-Aldrich, AC-15), anti-VEGF-A (R&D Systems, MAB293-SP), anti-VEGFR2 (R&D Systems, AF357), anti-pVEGFR2 (Cell Signaling, #2478, anti-phospho Tyr1175), anti-VEGFR3 (Santa Cruz Biotechnology, SC-321), anti-pVEGFR3 (Cell Applications, CY1115, anti-phospho-Tyr1230/1231), soluble VEGFR-3 (ReliaTech, RLT-S01-018-C050), anti-Cd31 (BD Bioscience, MEC13.3), anti-BrdU (Santa Cruz Biotechnology, SC-56258), anti-LYVE1 (AngioBio, 11-034), anti-podoplanin (Iowa Hybridoma Bank, 8.1.1) and anti-Tyr (Sigma-Aldrich, p5872). Sources of other reagents are as follows: Tamoxifen Free Base (MP Biomedicals), inhibitors for FGFR3 (PD 166866), VEGFR2 (Ki8751), VEGFR3 (MAZ51) and CXCR2 (SB225002) from Calbiochem. Tamoxifen (MP Biomedicals) was dissolved in Dimethyl sulfoxide (DMSO), mixed with sunflower seed oil, and intraperitoneally injected (final 1.5 mg) into pregnant females at E11.5 and 13.5. Adenoviruses expressing mouse Klf2 and human KLF4 were kindly provided Drs. Guillermo Garcia-Cardena (Harvard Medical School) and Chunming Liu (University of Kentucky College of Medicine), respectively.

Isolation of Mouse Embryonic Dermal LECs and Adult Lymph Node LECs

For isolation of embryonic dermal LECs, embryos were harvested at E16.5 and genotyped. Their back skins were then collected, chopped into pieces, and incubated with dispase and collagenase (1mg/ml, Hoffmann-La Roche, Ltd), collagenase II (50 U/mL, Worthington Biochemical, Lakewood, NJ) and DNase I (1,000 U/mL, New England Biolabs, Ipswich, MA) in phosphate buffered saline (PBS) at 37 °C for 1 hr. The enzymatically treated back skins were triturated through a needle (18.5G) to harvest dermal cell mixtures, which was filtered through a cell strainer, centrifuged, resuspended in EBM-based

culturing media, seeded on a culture dish, and incubated 37 °C. After 4 hr., the cells were washed twice with PBS, trypsinized, and incubated with an anti-LYVE1 rabbit antibody (Angiobio, 11-034) and an anti-Cd34 rat antibody (BD Pharmingen, 550537) at 4 °C for 1 hr. Mouse BECs were first collected using Dynabeads Sheep anti-Rat IgG and directly subjected to RNA isolation using Trizol reagents (Ambion). Next, mouse LECs were isolated from the remaining cell suspension using Dynabeads sheep anti-rabbit IgG and plated on a collagen pre-coated 6-well plate. For qRT-PCR, the cells were immediately subjected to RNA isolation without plating.

For isolation of adult lymph node LECs (LN-LECs), brachial, superficial cervical and axillary lymph nodes were harvested from Prox1-EGFP or Prox1-tdTomato mice and then incubated in DMEM with Penicillin/Streptomycin (2,000 U/mL) at 4 °C overnight. They were then incubated in a digestive enzyme solution (1 ml) in one well of 24-well plate, cut into small pieces with surgical scissors and incubated at 37 °C for 1 hour. The digestive enzyme solution is a mixture of dispase and collagenase (1 mg/ml, Hoffmann-La Roche, Ltd), collagenase II (50 U/mL, Worthington Biochemical, Lakewood, NJ) and DNase I (1,000 U/mL, New England Biolabs, Ipswich, MA) in PBS. The enzymatically treated lymph nodes were then triturated through an 18.5-gauge needle and the dissociated cells were filtered through a 40 µm-cell strainer. Subsequently, the cells were centrifuged and resuspended in media (EGMTM BulletKitTM with 20% FBS).

Gene and Protein Expression

Standard protocols were employed for quantitative real-time RT-PCR (qRT-PCR) and western blot assays. Nucleic acid sequences of primers, probes and siRNA duplexes will be available upon request. Plasmids and siRNA were transfected into primary endothelial cells using HMEC-L Nucleofector Kit (Lonza, VPB1003) and PBS¹, respectively. Sequences of siRNA are KLF2 (#1, CCAAGAGUUCGCAUCUGAATT; #2, AGACCUACACCAAGAGUUCUU), KLF4 (#1, GGACUUUAUUCUCUCCAAUdTdT; #2, CCUUACACAUGAAGAGGCAdTdT), FGFR3 (#1,

CACGACCUGUACAUGAUCAdTdT; #2, UGCACAACCUCGACUACUAdTdT), ORAI1 (#1, UCACUGGUUAGCCAUAGA; #2, GCUCACUGGUUAGCCAUAdTdT). Protein concentration of VEGF-A and VEGF-C was determined using Human VEGF Standard ELISA Development Kit (Peprotech) and Human VEGF-C ELISA Kit (AbCam). Whole-mount and tissue section immunofluorescent staining of mouse tissues were performed as previously described ².

Cell Proliferation and Death Assays

5-Bromo-2'-deoxyuridine (BrdU, Sigma-Aldrich Co.)-based cell proliferation assay was performed as previously described ³. Briefly, BrdU (final 100 μ M) was added to the culture media 2 hr. prior to harvest. Cells were detached using Trypsin-EDTA, fixed in ethanol (70%) for 4 hr. at - 20°C and subjected to the standard BrdU assay. Cell death assay was performed using Cell Death Detection ELISA (Roche). Source of chemical inhibitors for VEGFRs, FGFRs and CXCR2 were previously described ⁴. SKF 96365 hydrochloride and Bapta-AM were purchased from Tocris Bioscience and Sigma-Aldrich, respectively.

Chromatin Immunoprecipitation (ChIP) assays

ChIP assay was performed as previously described ⁴. Sequences of the primers used for the following ChIP assays are as follows: VEGF-C 210-kb UPS (CCCTCTCCAACTGGATTTC/ATCGGACATTTTGCAAGACC), VEGF-C 130-kb UPS (GACCTGAAAGGACCTGTGGC/TGGCTAACAGGAAACCCTCC), VEGF-C 50-kb UPS (ATTGCACAAGGCCAAAATC/GCCTACTGTGCTTGCATTGA), FGFR3 34-kb UPS (GGGACTTCCCACACTCGTAA/GCCTCAGTGTACCCGTCTGT), p57 (CAGGCTCACCTGAGATAGGG/CAGGCCAGACCAAAGAGAC).

Confocal laser-scanning fluorescence microscopy for calcium imaging

Human primary LECs were transiently transfected on μ -Slides (Ibidi GmbH, Germany) with a GCaMP3-expressing vector for 24 hr. and then exposed to steady laminar flow (2 dyne/cm²) generated with a syringe pump using either culturing media with or without SKF-96365 (10 μ M), or PBS lacking Ca²⁺ and Mg²⁺. Calcium signals were captured using a Leica TCS SP5 AOTF MP confocal microscope system (Leica Microsystems, Germany). Florescent images were collected in time series (*xyt*, 1 s per frame) with the Leica LAS AF imaging software and fluorescence intensity was determined by the Leica LAS lite.

SUPPLEMENTAL INFORMATION REFERENCES

1. Kang J, Ramu S, Lee S, Aguilar B, Ganesan SK, Yoo J, Kalra VK, Koh CJ, Hong YK. Phosphate-buffered saline-based nucleofection of primary endothelial cells. *Anal Biochem.* 2009;386:251-255
2. Choi I, Chung HK, Ramu S, Lee HN, Kim KE, Lee S, Yoo J, Choi D, Lee YS, Aguilar B, Hong YK. Visualization of lymphatic vessels by Prox1-promoter directed GFP reporter in a bacterial artificial chromosome-based transgenic mouse. *Blood.* 2011;117:362-365
3. Takeyoshi M, Yamasaki K, Yakabe Y, Takatsuki M, Kimber I. Development of non-radio isotopic endpoint of murine local lymph node assay based on 5-bromo-2'-deoxyuridine (BrdU) incorporation. *Toxicol Lett.* 2001;119:203-208
4. Choi I, Lee S, Kyoung Chung H, Suk Lee Y, Eui Kim K, Choi D, Park EK, Yang D, Ecoiffier T, Monahan J, Chen W, Aguilar B, Lee HN, Yoo J, Koh CJ, Chen L, Wong AK, Hong YK. 9-cis retinoic Acid promotes lymphangiogenesis and enhances lymphatic vessel regeneration: therapeutic implications of 9-cis retinoic Acid for secondary lymphedema. *Circulation.* 2012;125:872-882

ONLINE FIGURE LEGENDS**Online Figure I. Cellular, molecular and biochemical effects of laminar flow at various shear**

force levels on cultured LECs. Primary human LECs were subjected to steady laminar flow at 0, 0.25, 0.5, 1, 2, or 5 dyne/cm². **(A)** Cellular morphology change was imaged at 0 (static), 6, 12 and 24 hr. under the flow. Scale bars: 50 μm. **(B-C)** qRT-PCR assays showing the expression levels of KLF2 **(B)** and KLF4 **(C)** in LECs that were subjected to laminar flow at various forces for 24 hr. **(D)** Intracellular calcium influx was measured in LECs that were plated on μ-slides (Ibidi, GmbH), loaded with Fluo-4 and subjected to laminar flow at the indicated force levels. **(E-H)** qRT-PCR assays showing the expression levels of VEGF-A **(E)**, VEGF-C **(F)**, FGFR3 **(G)**, and p57 **(H)** in LECs after exposure to the indicated levels of laminar flow for 24 hr. All qRT-PCR expression levels were normalized against the level of β-actin. Error bars: the standard deviations (SD) of the mean. Statistical values: *, p < 0.05; **, p < 0.01; ***, p < 0.001.

Online Figure II. Prox1 expression was not altered in LECs by steady laminar flow at 2 dyne/cm².

Human primary LECs were subjected to steady laminar flow at 2 dyne/cm² for the indicated time. PROX1 mRNA levels were quantified using qRT-PCR and normalized against the level of β-actin. Error bars: the standard deviations (SD) of the mean.

Online Figure III. Activation of proliferation of human and mouse LECs by laminar flow.

(A) Human primary LECs were exposed to steady laminar flow at 0, 0.25, 0.5, 1, 2, or 5 dyne/cm² for 24 hr. and cell proliferation was measured by BrdU-incorporation assay. Percent BrdU-positive cells are shown against the static (0 dyne/cm²) culture. **(B)** LECs freshly isolated from lymph nodes of adult mice were subjected or not to steady laminar flow (LF, 5 dyne/cm²) for 24 hr. and the relative amount of cells in the S-phase was determined by flow cytometry. Error bars: the standard deviations (SD) of the mean. Statistical values: *, p < 0.05; **, p < 0.01; ***, p < 0.001.

Online Figure IV. ORAI1 is essential for the laminar flow-induced gene regulation in LECs. (A-F)

Mouse dermal LECs were freshly isolated from the back skin of wild type embryos (E16.5) and cultured. After 2 days, culture media were changed with fresh media containing PBS (CTR) or SKF-96365 (SKF, 10 μ M) before laminar flow (LF, 2 dyne/cm²) was applied or not for 24 hr. Subsequently, qRT-PCR was performed to determine the expression levels of p57 (A), VEGF-A (B), VEGF-C (C), FGFR3 (D), KLF2 (E), AND KLF4 (F). (G-M) Human primary dermal LECs were transfected overnight with control siRNA (siCTR) or a second set of ORAI1 siRNA (siORAI1-2), which is different from the first set (siORAI1-1) used for Figs.3 & 4. Cells were then subjected to static culturing or laminar flow (LF, 2 dyne/cm²) for 24 hr. before qRT-PCR analyses. Relative expression levels of ORAI1 (G), KLF2 (H), KLF4 (I) VEGF-A (J), VEGF-C (K), FGFR3 (L), and p57 (M) were normalized again β -actin and expressed in the graphs. Error bars: the standard deviations (SD) of the mean. Statistical values: **, p < 0.01; ***, p < 0.001.

Online Figure V. Laminar flow-activated calcium influx in LECs is inhibited by SKF-96365.

Time-lapse images (A) and relative signal intensity graph (B) showing the intracellular calcium mobilization in LECs upon the onset of steady laminar flow (LF) at 2 dyne/cm². Calcium influx was detected by the calcium reporter protein, GCaMP3. LECs were transfected with a GCaMP3-expressing vector for 24 hr. and then exposed to laminar flow using culture media (CTR), culture media containing SKF-96365 (SKF, 10 μ M), or PBS without (w/o) Ca²⁺ and Mg²⁺. Error bars: the standard deviations (SD) of the mean. Statistical values: *, p < 0.05; **, p < 0.01; ***, p < 0.001.

Online Figure VI. Orai1 is required for the regulation of the laminar flow-responsive genes in mouse LECs.

Mouse dermal LECs were freshly isolated from wild type (WT) or Orai1 KO mutant embryos and subjected or not to laminar flow (LF, 2 dyne/cm²) for 24 hr. qRT-PCR assays were performed to determine the expression levels of Klf2, Klf4, Vegf-A, Vegf-C, Fgfr3, and p57. Error bars: the standard deviations (SD) of the mean. Statistical values: *, p < 0.05; **, p < 0.01; ***, p < 0.001.

Online Figure VII. Quantitation of the lymphatic density in the control and mutant embryos.

Relative lymphatic area was determined in the wild type and various mutant embryos. **(A,B)** Relative lymphatic vessel area in the embryonic back skins **(A)** and young adult trachea **(B)** of *Orai1* heterozygote (Prox1-tdTomato; *Orai1* Het) and KO (Prox1-tdTomato; *Orai1* KO) animals shown in Fig.5. **(C,D)** Relative lymphatic vessel area in the embryonic back skins of wild type and KO embryos lacking *Klf2* **(C)** or *Klf4* **(D)**, as shown in Fig.7 **(A,C)** and **(E,H)**, respectively.

Online Figure VIII. Expression of laminar flow-responsive genes is dysregulated in the isolated mouse LECs from *Orai1* KO embryo.

qRT-PCR analyses showing the mRNA level of *Vegf-A* **(A)**, *Vegf-C* **(B)**, *Klf2* **(C)**, *Klf4* **(C)**, *Fgfr3* **(E)** and *p57* **(F)** in primary embryonic LECs (mLECs) and BECs (mBECs) that were freshly isolated using anti-Lyve1 and anti-Cd34 antibodies, respectively, from *Orai1* wild type embryos (WT, n=4) or littermate KO embryos (KO, n=4) (E16.5). Expression of each gene was measured and normalized against that of β -actin. Each data point was derived from one embryo. Results were expressed as mean and the standard error of the mean (SEM). Statistical values: *, $p < 0.05$; **, $p < 0.01$; ***, $p < 0.001$; n.s., not significant.

Online Figure IX. KLF2 and KLF4 is necessary for the regulation of the laminar flow-responsive genes in LECs.

(A-D) qRT-PCR data showing the effects of knockdown of *KLF2* **(A,B)** or *KLF4* **(C,D)** on the expression of *KLF2*, *KLF4*, *VEGF-A*, *VEGF-C*, *FGFR3* and *p57* in LECs exposed to laminar flow. Knockdown was performed with two different siRNAs for *KLF2* (siKLF2-1 **(A)** and siKLF2-2 **(B)**), or two different siRNAs for *KLF4* (siKLF4-1 **(C)** or siKLF4-2 **(D)**), along with control siRNA (siCTR) for 24hr. prior to the onset of laminar flow (2 dyne/cm²) for 24 hr. **(E)** Mouse dermal LECs were freshly isolated from wild type (WT) and *Klf2* KO mutant embryos and then subjected or not to laminar flow (LF, 2 dyne/cm²) for 24 hr. qRT-PCR assays were performed to determine the expression levels of *VEGF-A*, *VEGF-C*, *FGFR3* and *p57*. **(F)** qRT-PCR assays showing the knockdown efficiency of *KLF2* and *KLF4*

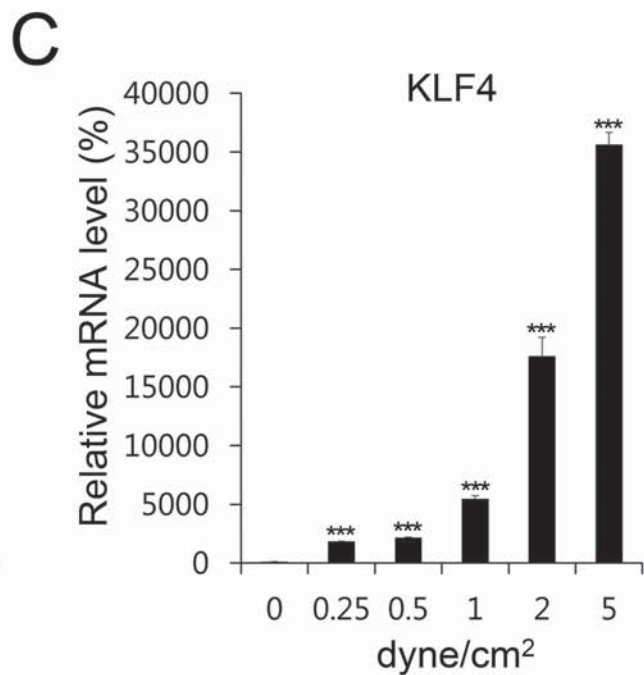
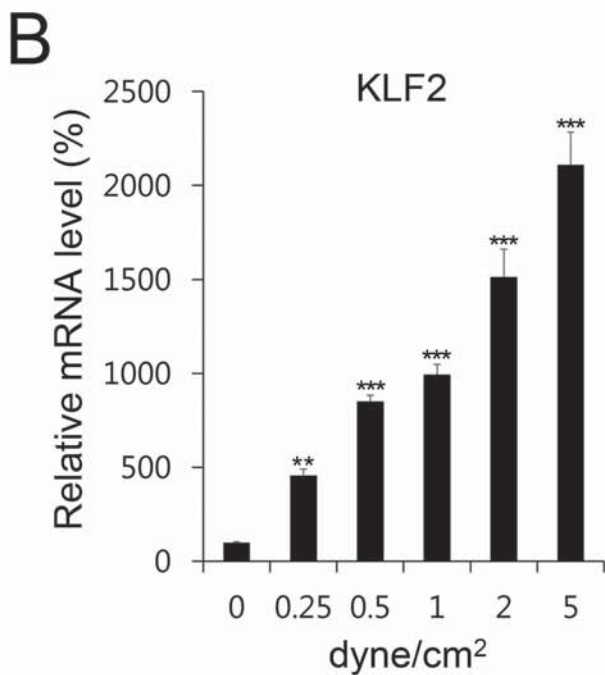
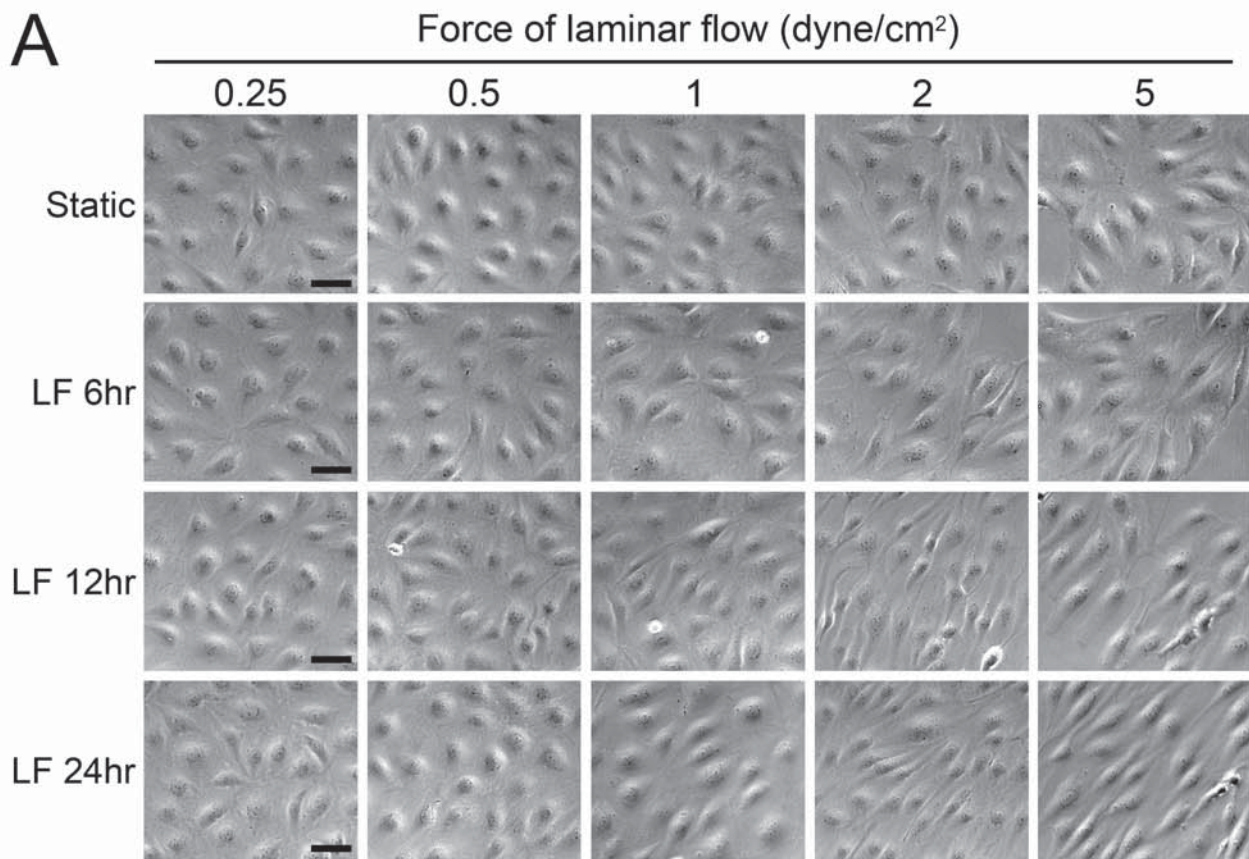
in the experiments of Fig.6A. Error bars: the standard deviations (SD) of the mean. Statistical values: *, $p < 0.05$; **, $p < 0.01$; ***, $p < 0.001$.

Online Figure X. Relative locations of the putative enhancers of VEGF-C and FGFR3. Red boxes mark the putative upstream sequences (UPS) that may function as enhancers in VEGF-C and FGFR3. Binding of KLF2 and KLF4 to these regions were determined by CHIP assays shown in Fig.6D. The transcriptional start site, the direction of the coding sequences (CDS) as well as the ENCODE histone tracks (H3K4Me1, H3K27Ac and H3K4Me3) are also shown.

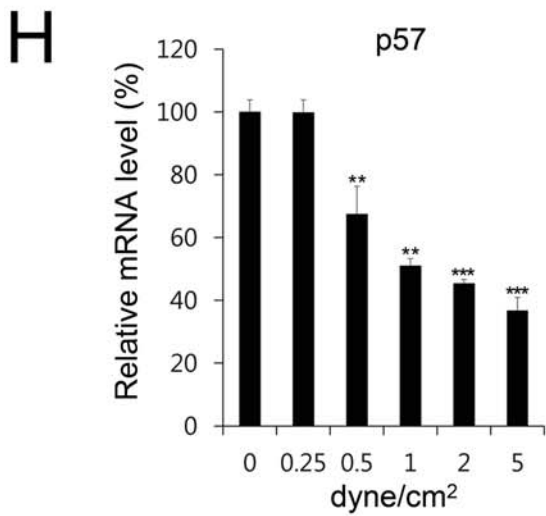
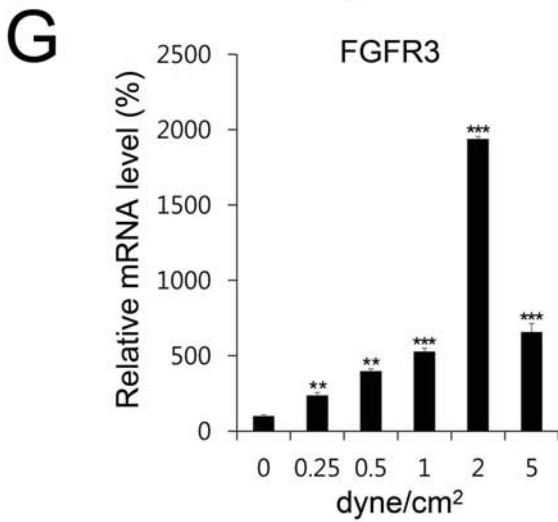
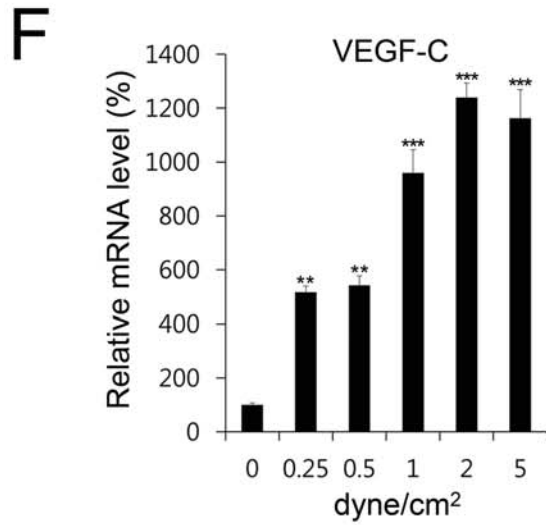
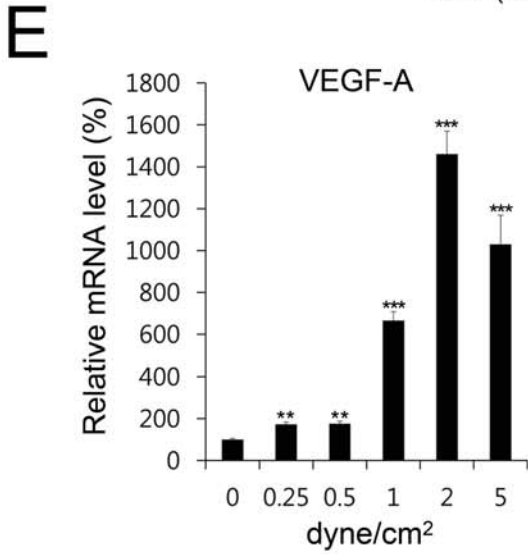
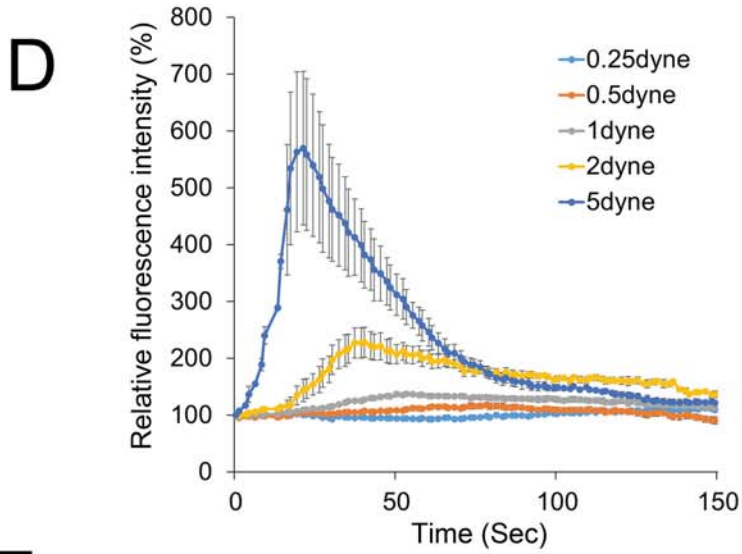
Online Figure XI. Overexpression KLF2 and KLF4 rescues the compromised flow-induced gene expression pattern caused by Orai1 knockdown. LECs were transfected with control siRNA (siCTR) or ORAI1 siRNA (siORAI1-1) overnight, infected simultaneously with control adenovirus (C) or with Ade-KLF2/ Ade-KLF4 (2/4), and followed by static culturing or laminar flow (2 dyne/cm²) for 24 hr. before qRT-PCR analyses. Relative expression levels of VEGF-A (A), VEGF-C (B), FGFR3 (C), p57 (D) ORAI1 (E), KLF2 (F), and KLF4 (G) were normalized again β -actin and expressed in the graphs. Error bars: the standard deviations (SD) of the mean. Statistical values: **, $p < 0.01$; ***, $p < 0.001$, n.s., not significant.

Online Figure XII. Low-power images of the back skin of wild type, *Klf2*^{ECKO}, and *Klf4*^{ECKO} embryos. (A) The images of developing dermal lymphatic and blood vessels in the control embryos (*Klf2*^{+/+}; *Cdh5(PAC)-CreER^{T2}*) or endothelial-specific inducible *Klf2* KO embryos (*Klf2*^{fl/fl}; *Cdh5(PAC)-CreER^{T2}*) at E15.5. Lymphatic and blood vessels were stained with anti-Lyve1 and anti-Cd31 antibodies, respectively. (B) Dermal lymphatic and blood vessels were visualized in the control embryos (*Klf4*^{+/+}; *Prox1-CreER^{T2}*; *Prox1-tdTomato*) or lymphatic-specific *Klf4* KO embryos (*Klf4*^{fl/fl}; *Prox1-CreER^{T2}*; *Prox1-tdTomato*) at E15.5. Lymphatic vessels were visualized using the tdTomato reporter and blood vessels were stained with anti-Cd31 antibody. Scale bars: 100 μ m.

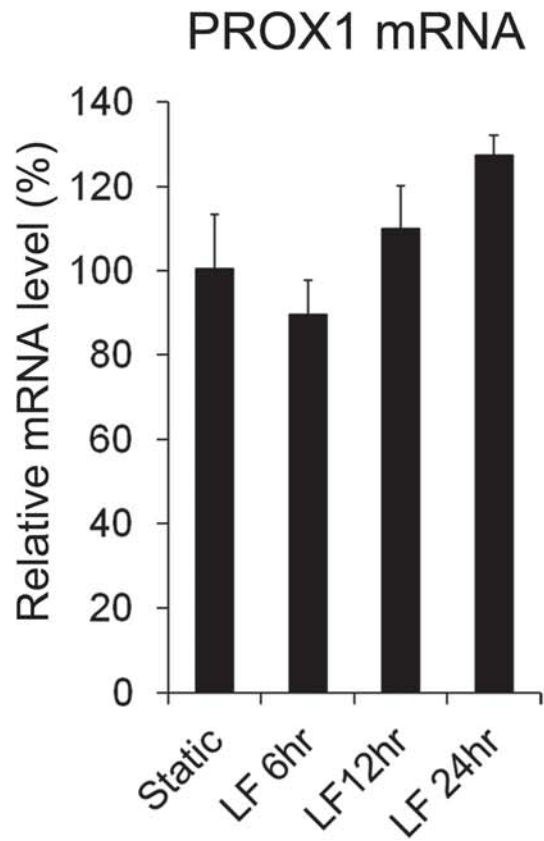
Online Figure XIII. Working model for the laminar flow-induced LEC proliferation. Low-rate steady laminar flow activates ORAI1, which increases the intracellular calcium influx and upregulates KLF2 and KLF4 in LECs. Increased KLF2 and KLF4 proteins individually and/or concertedly stimulate the gene expression of VEGF-A, VEGF-C and FGFR3, and suppress the p57 expression, promoting LEC proliferation and survival.



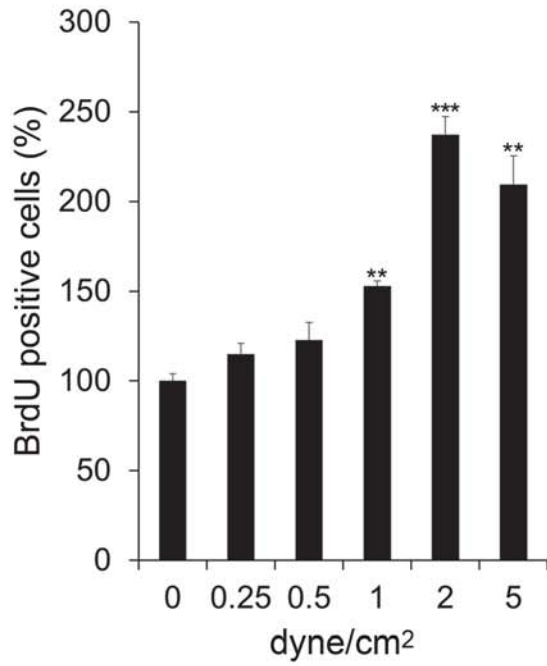
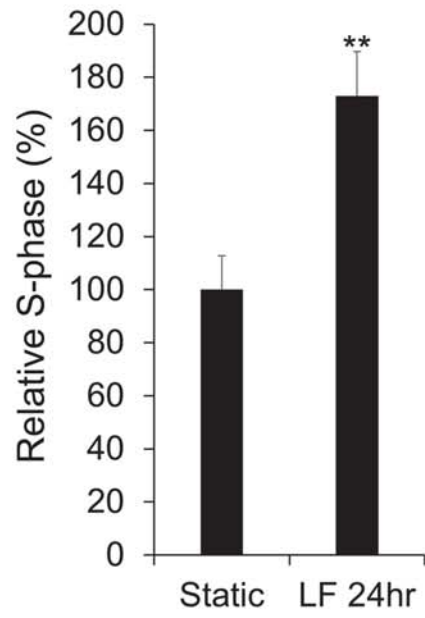
Online Figure I (Part1)



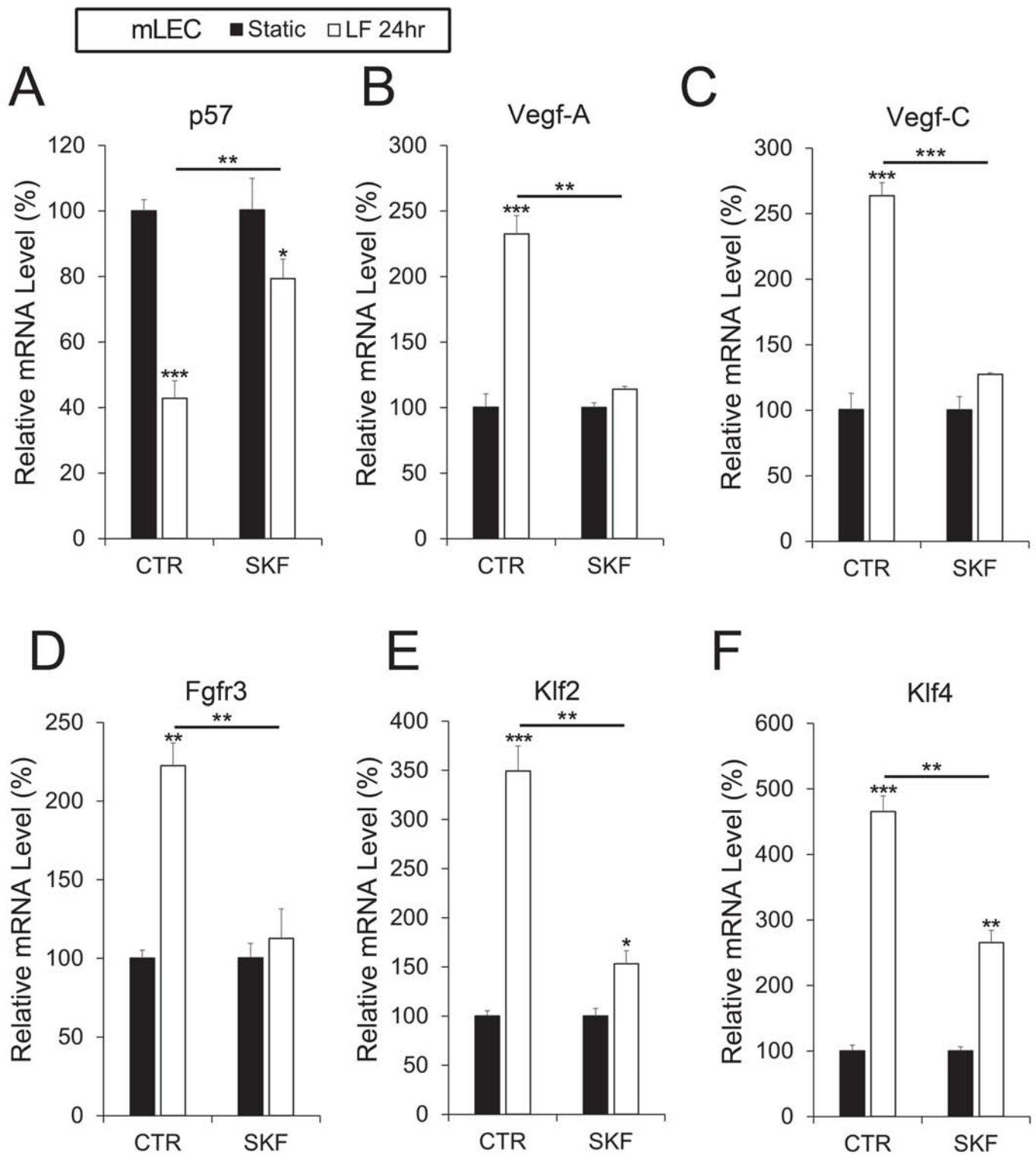
Online Figure I (Part2)



Online Figure II

A**B**

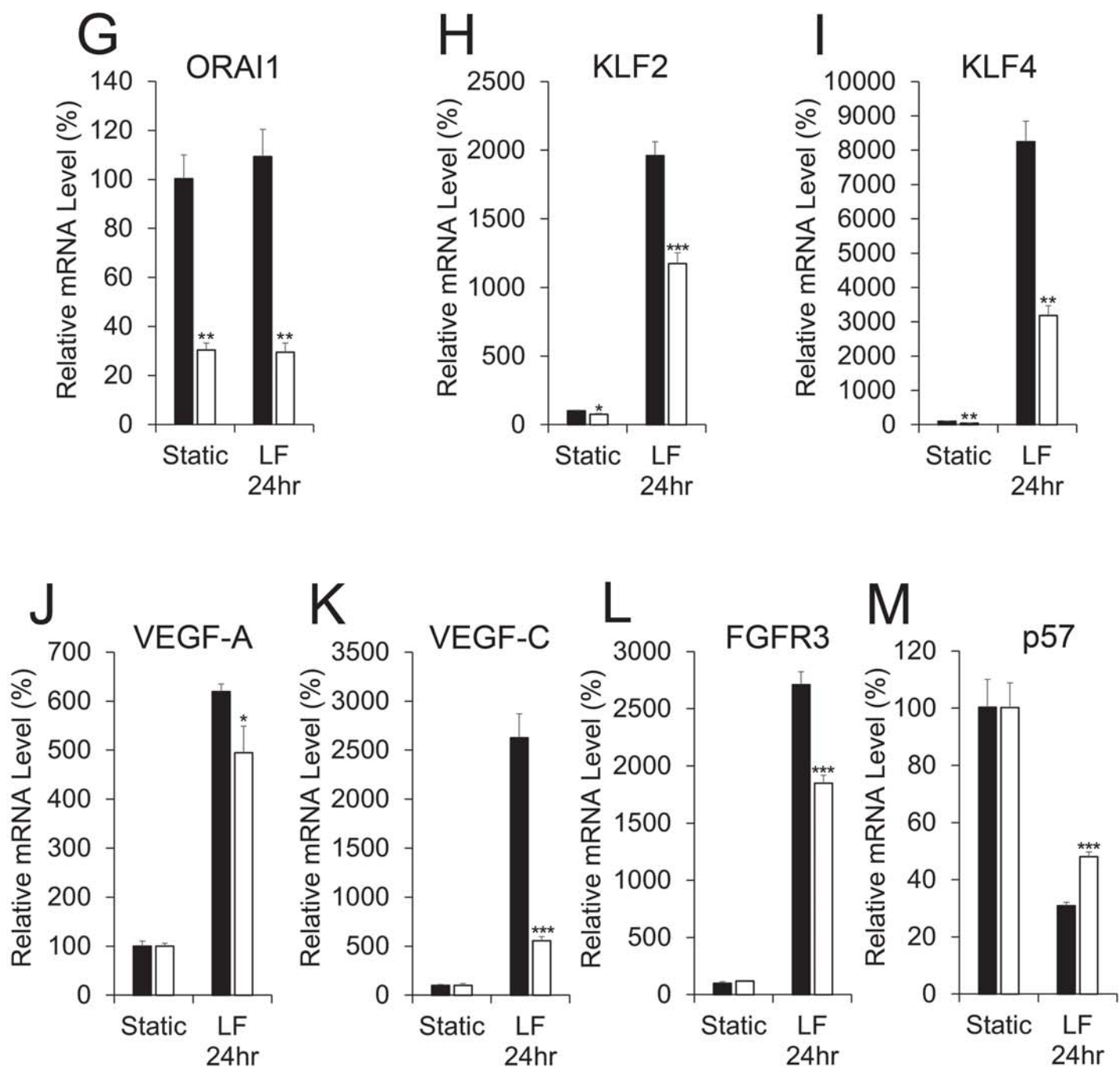
Online Figure III



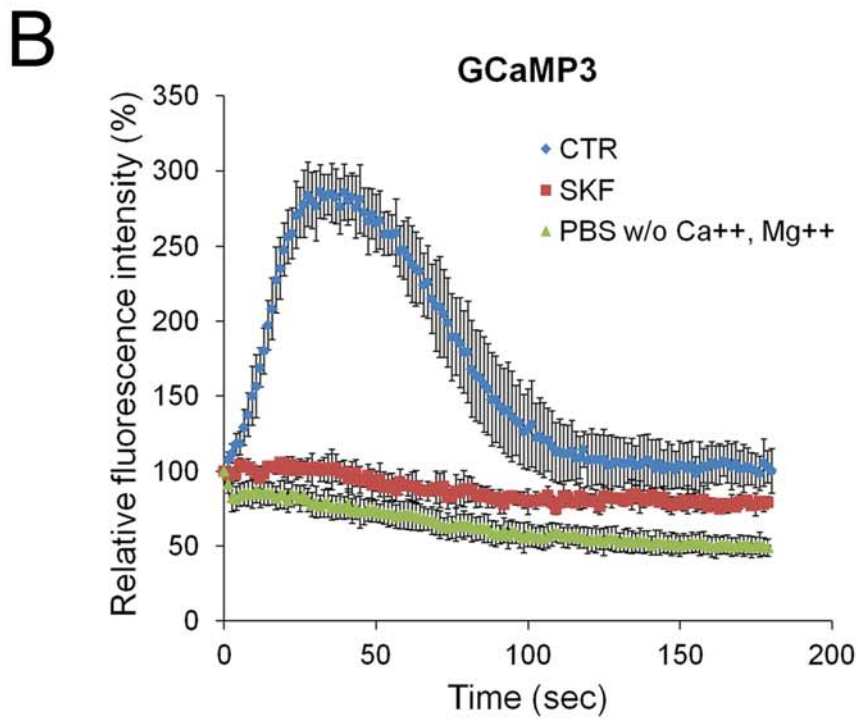
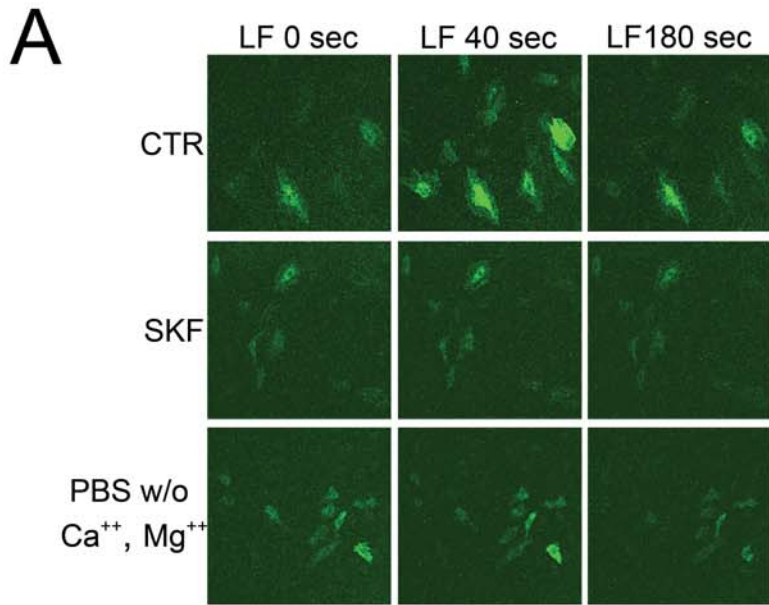
Online Figure IV (Part1)

ORAI1 knockdown in LEC

■ siCTR □ siORAI1-2

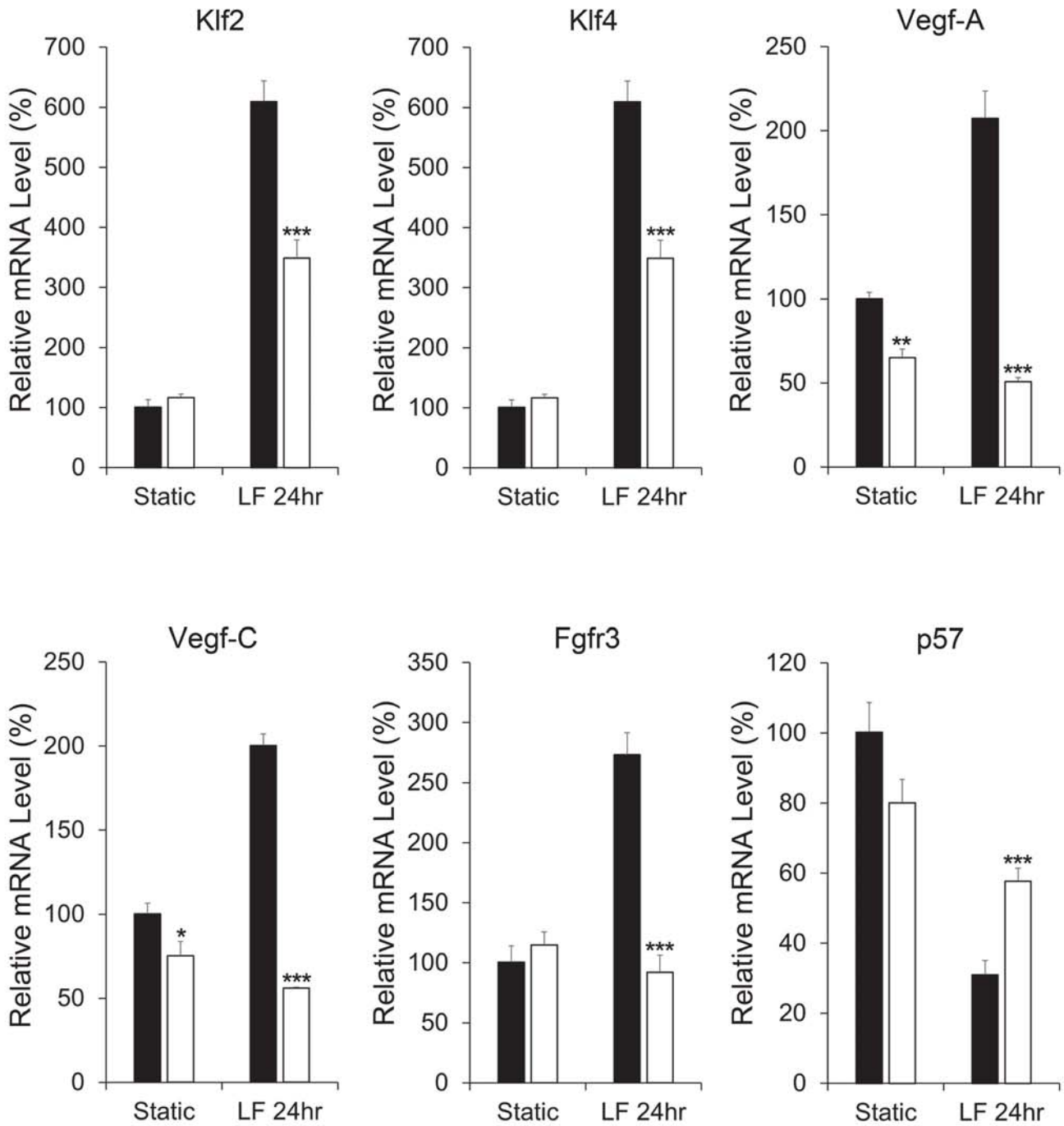


Online Figure IV (Part2)

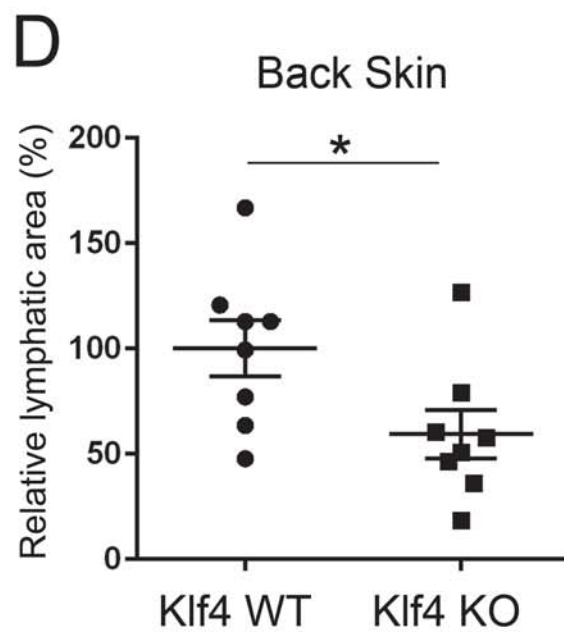
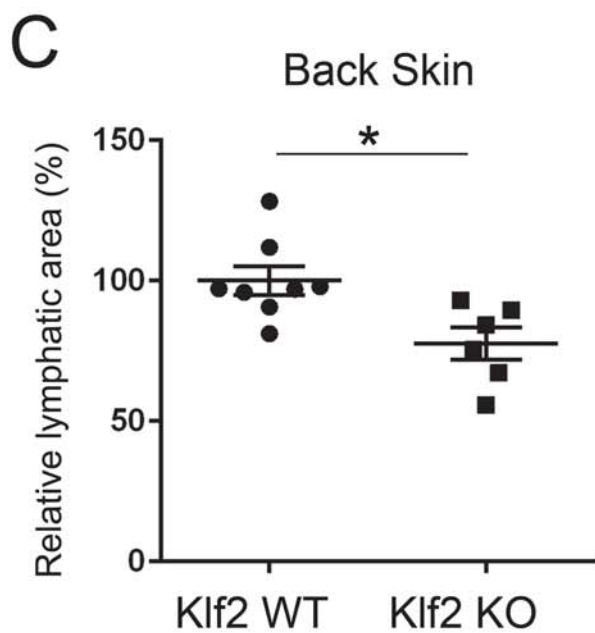
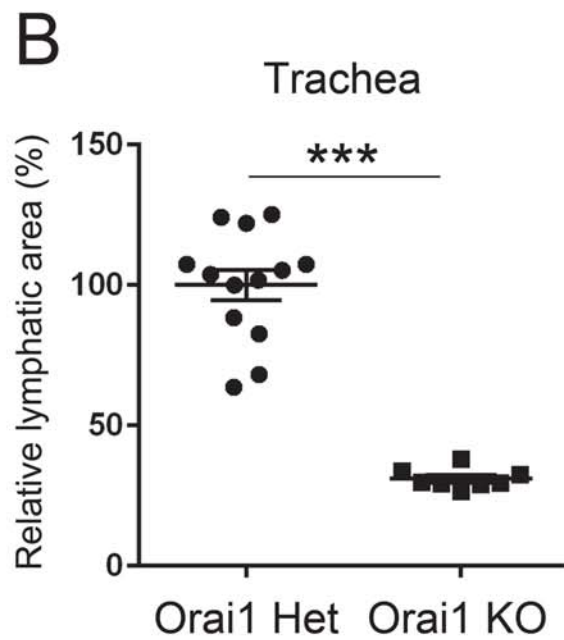
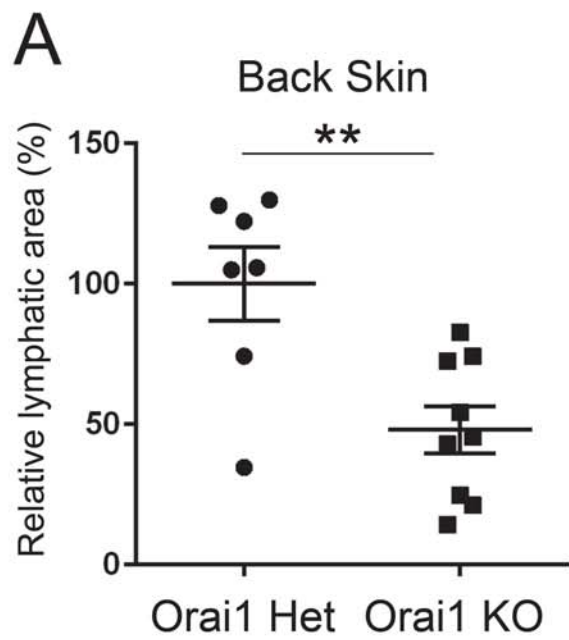


Online Figure V

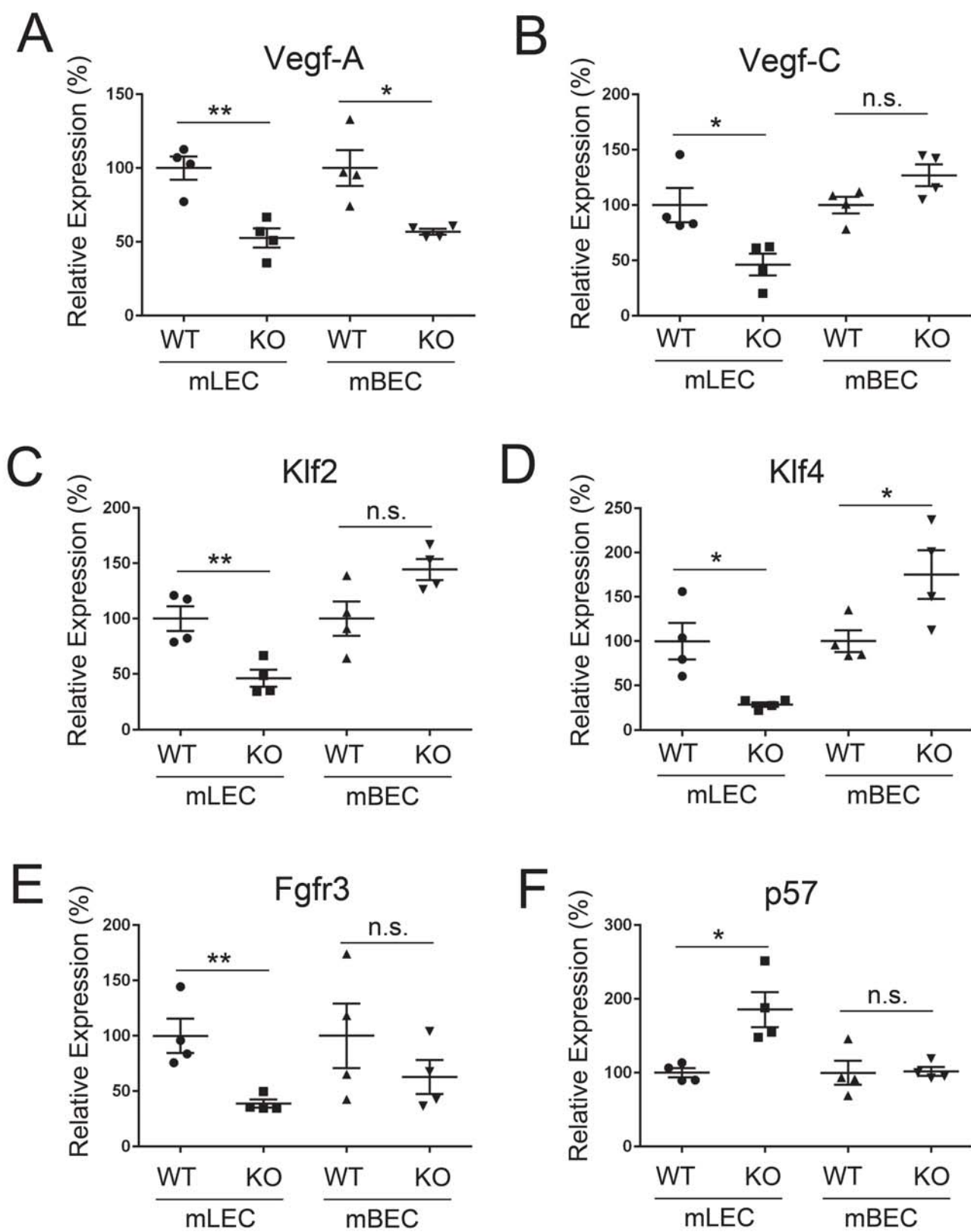
Orai1 WT vs KO mLEC ■ WT □ KO



Online Figure VI



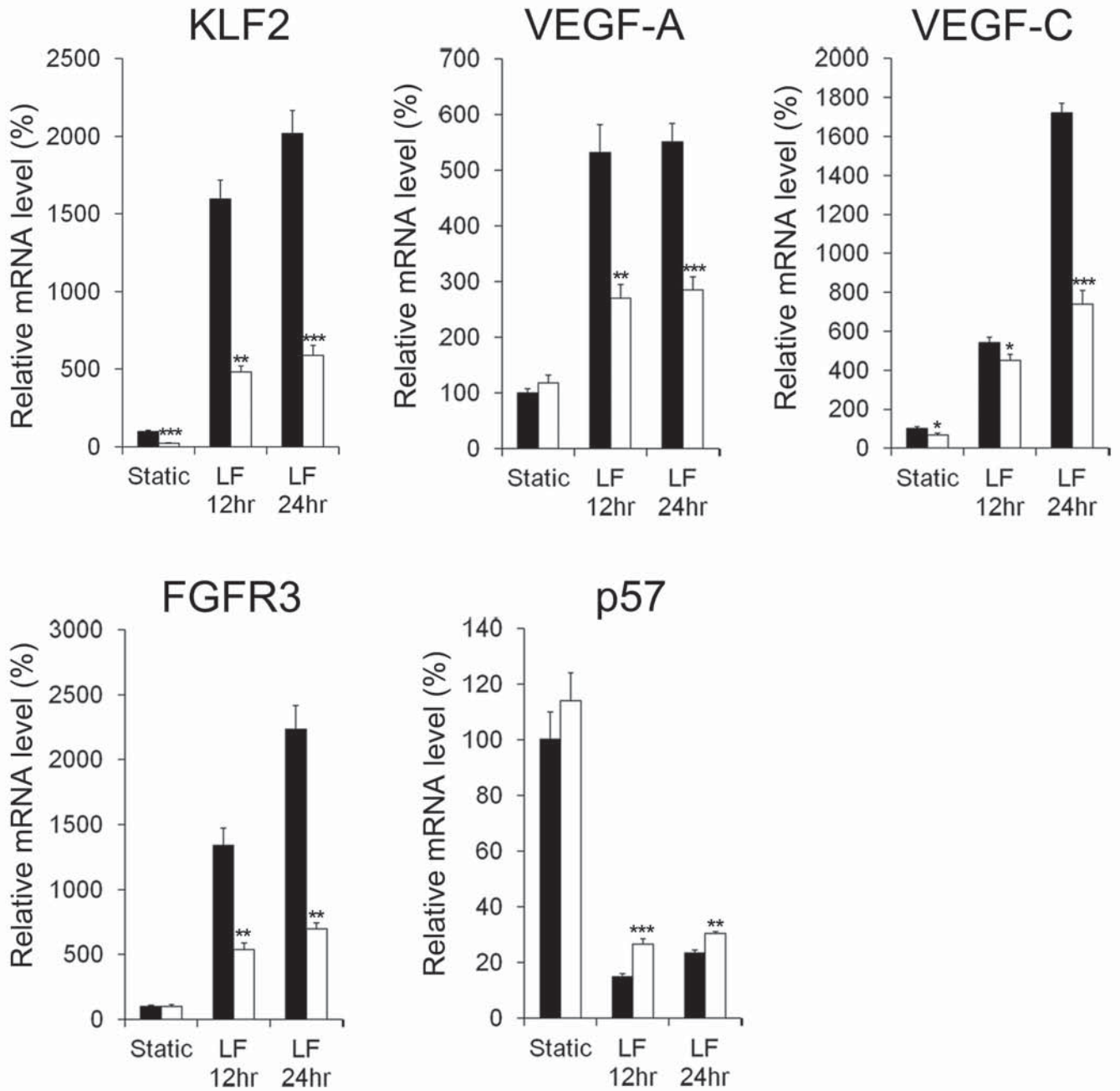
Online Figure XII



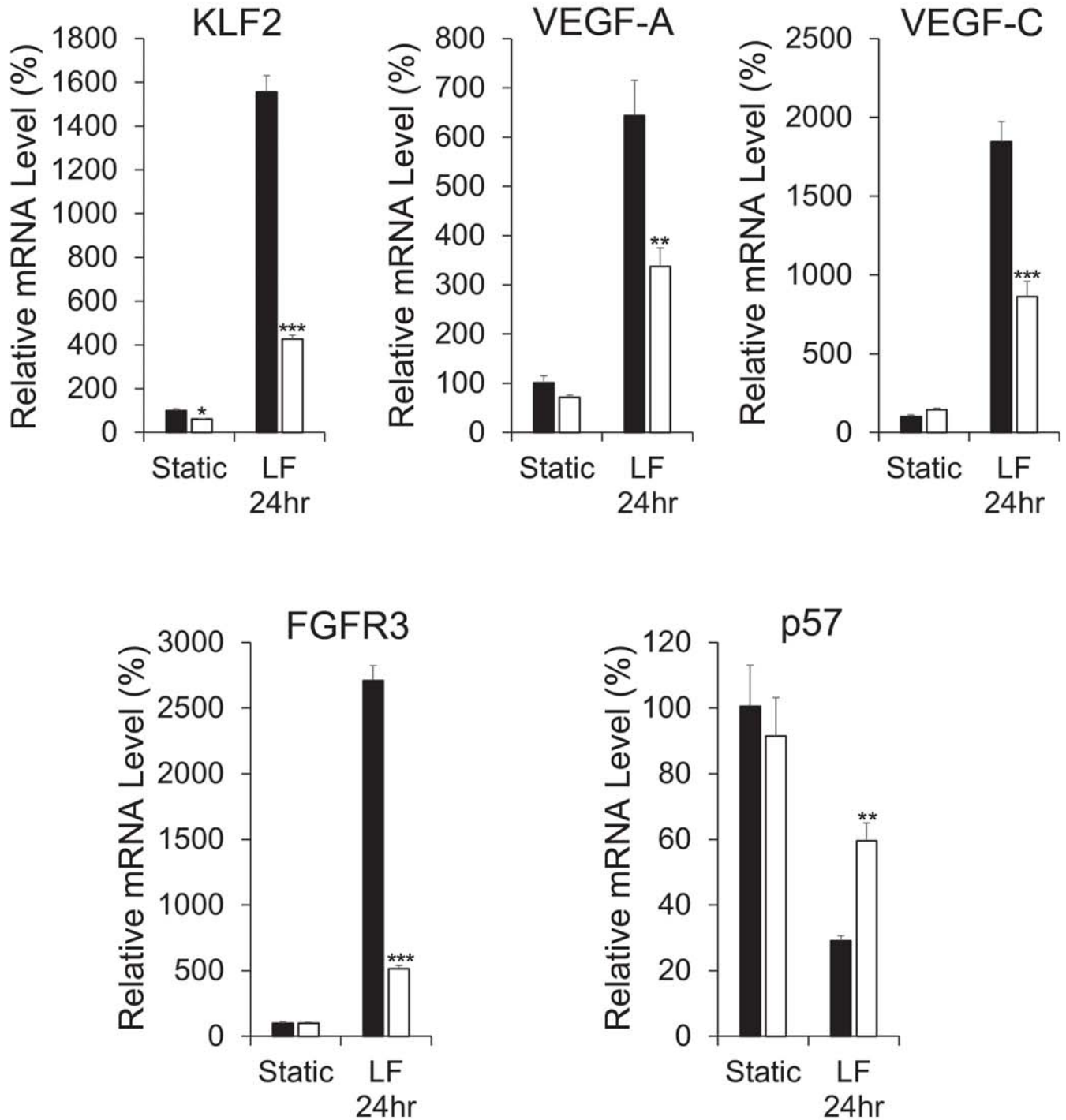
Online Figure VIII

A

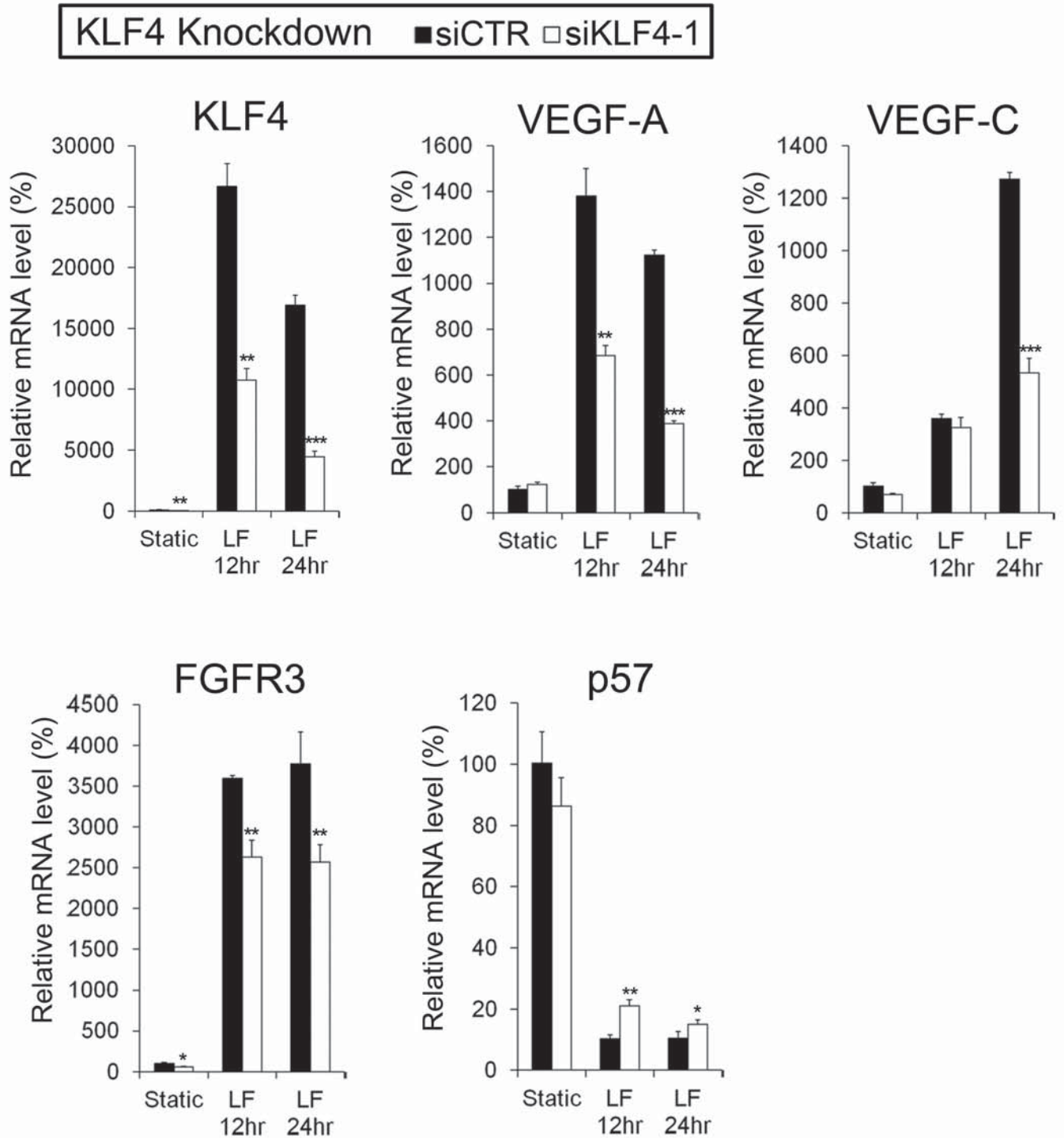
KLF2 Knockdown ■ siCTR □ siKLF2-1



Online Figure IX (Part1)

B**KLF2 Knockdown** ■ siCTR □ siKLF2-2**Online Figure IX (Part2)**

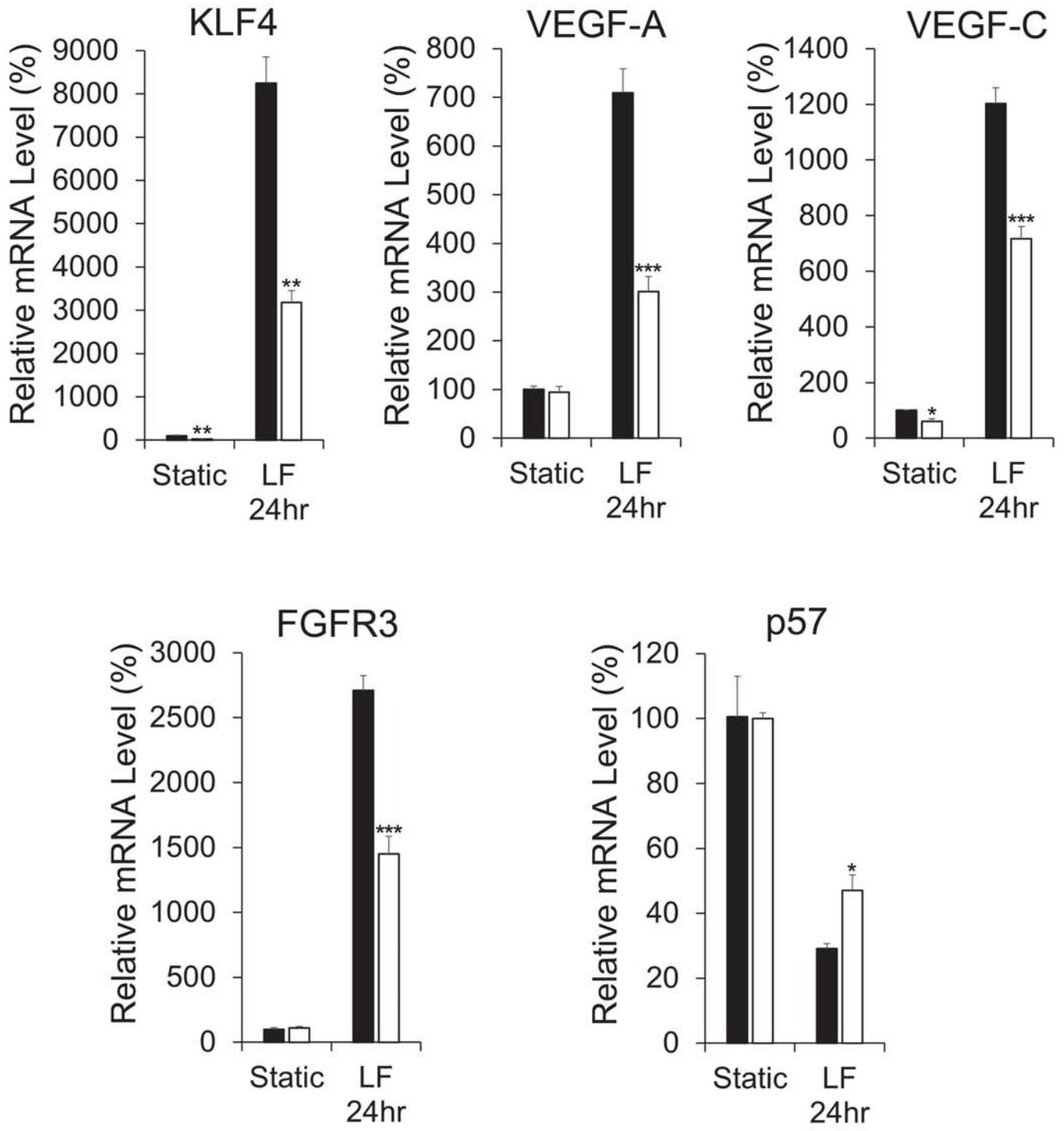
C



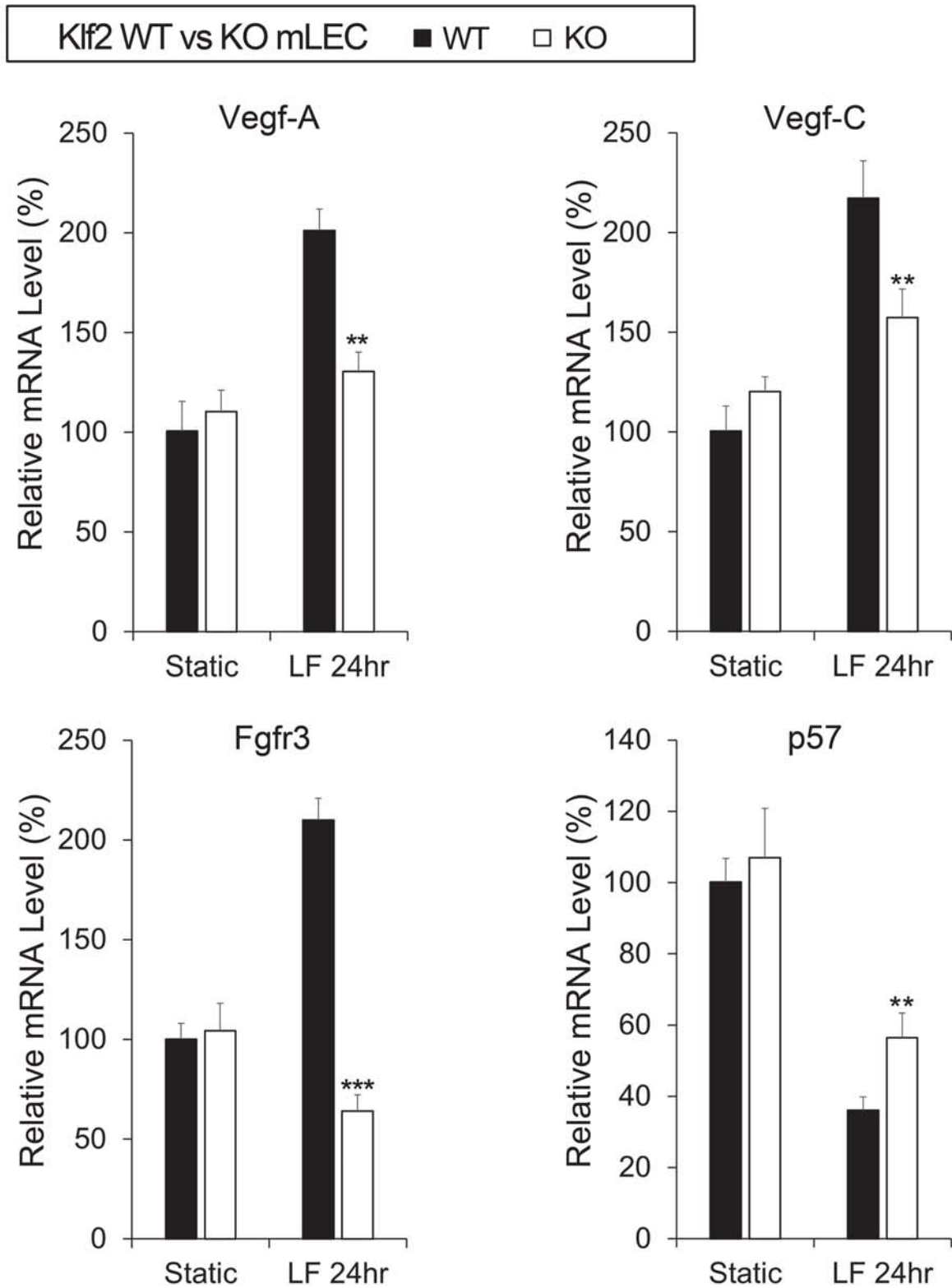
Online Figure IX (Part3)

D

KLF4 Knockdown ■ siCTR □ siKLF4-2

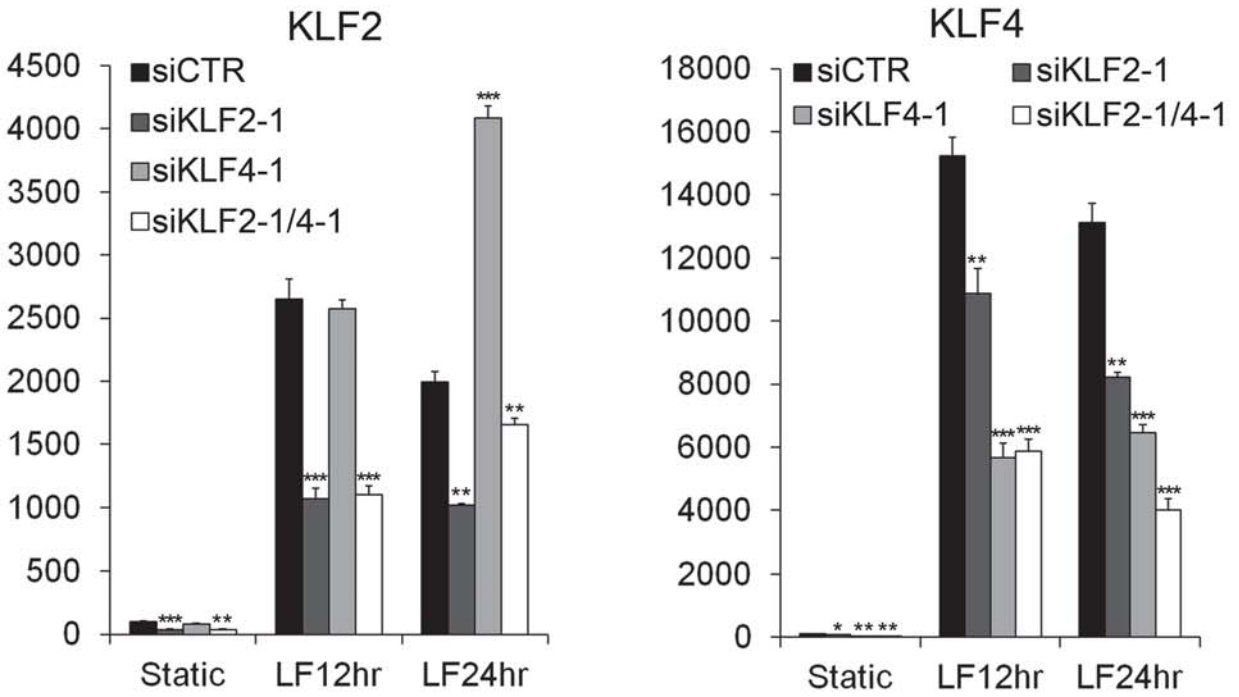


Online Figure IX (Part4)

E

Online Figure IX (Part5)

F

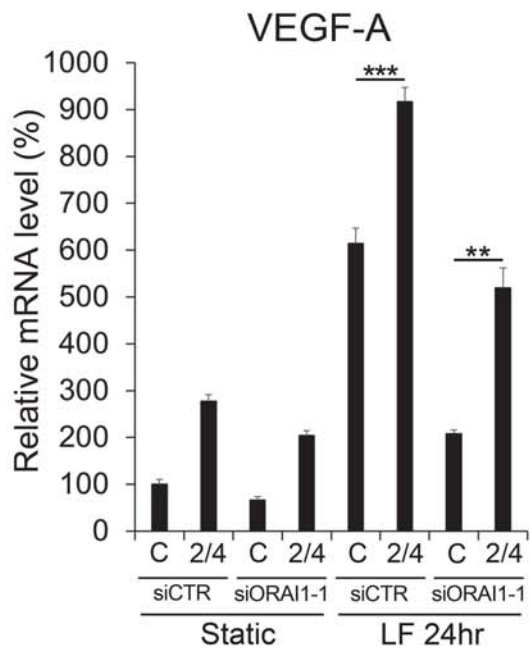
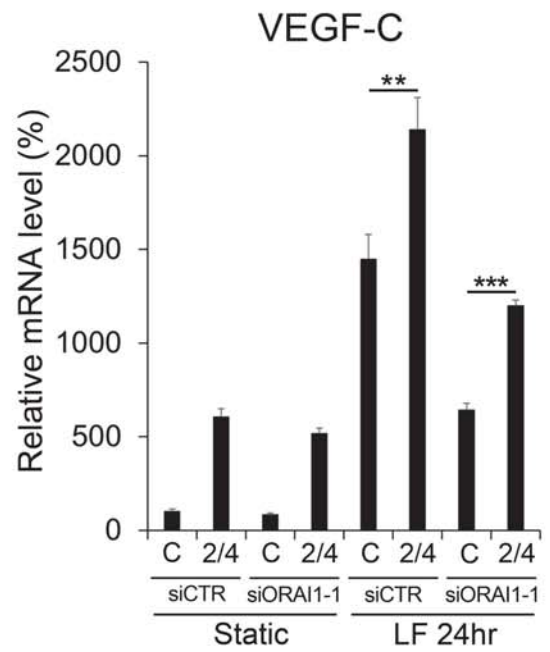
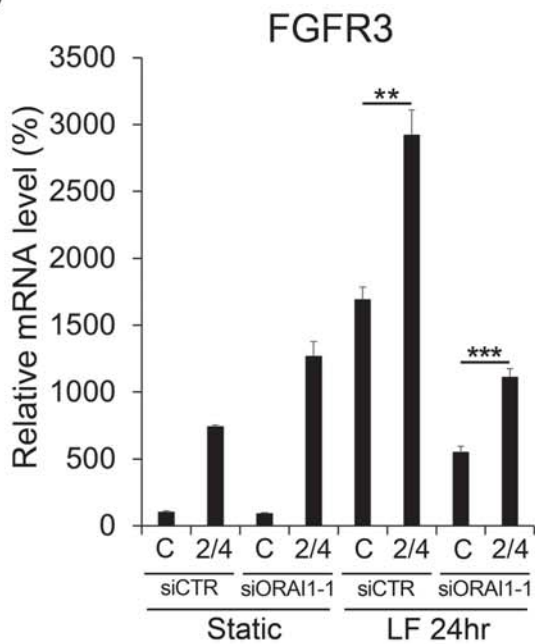
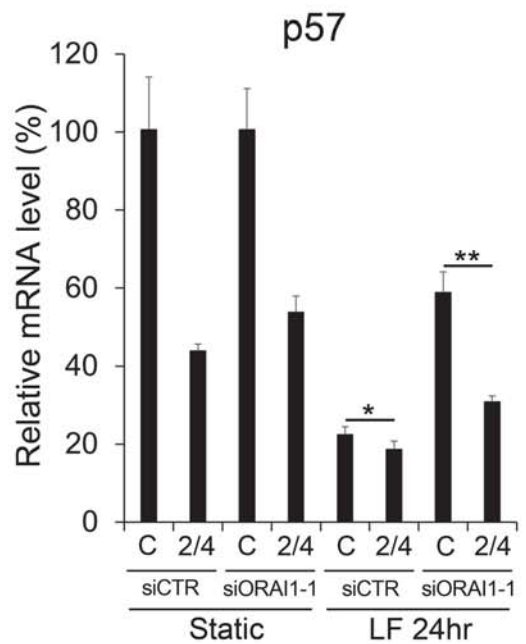


Online Figure IX (Part6)

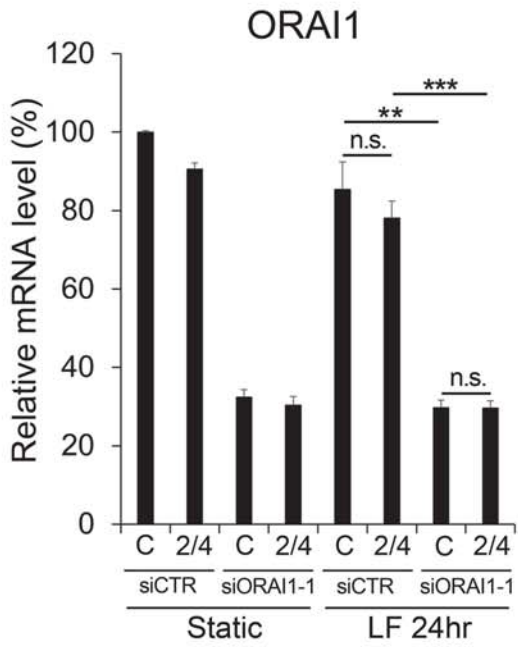
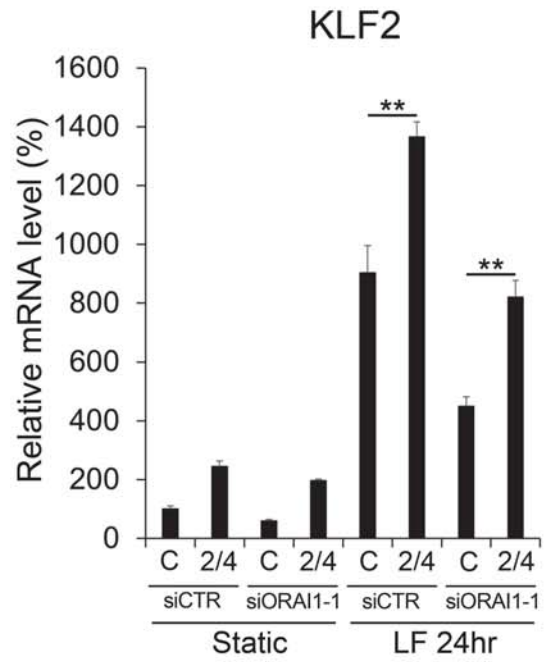
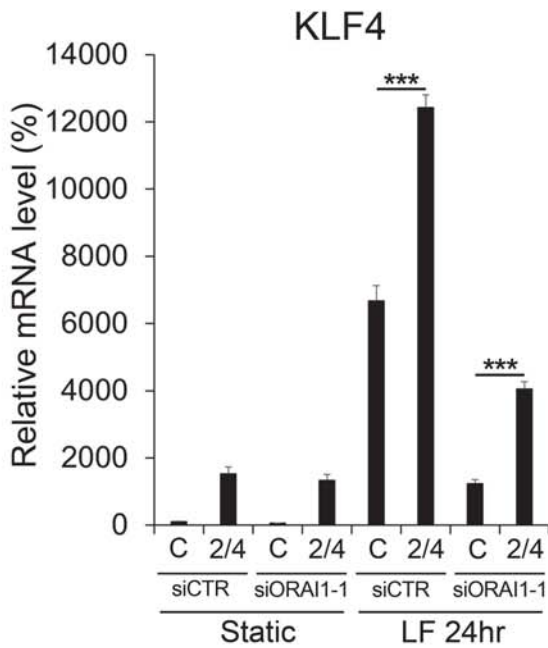
UCSC Genome Browser hg18 Assembly



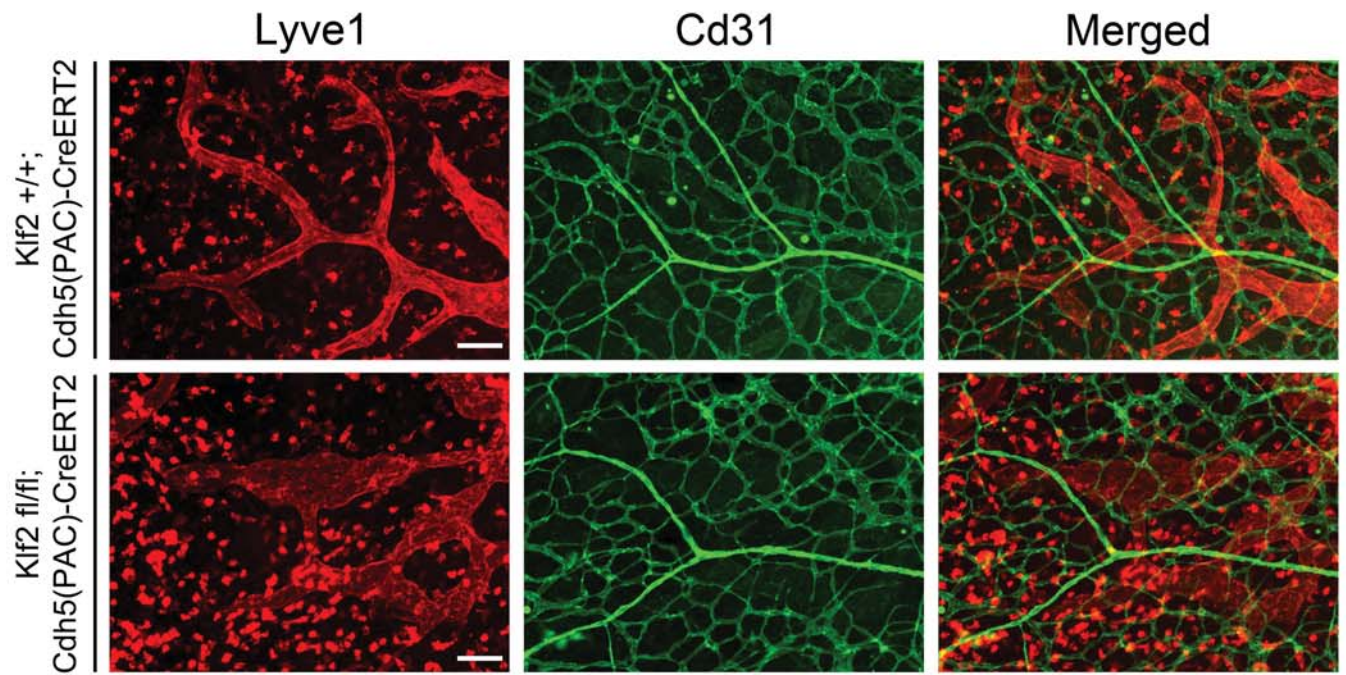
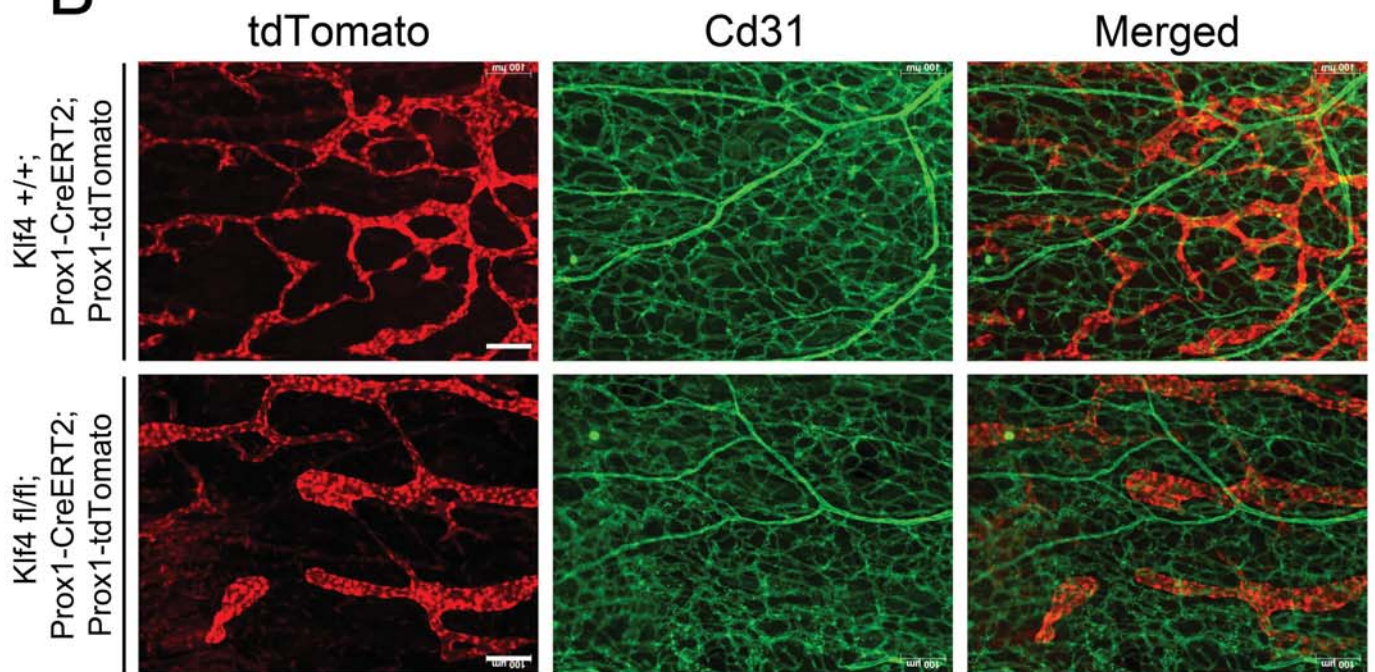
Online Figure X

A**B****C****D**

Online Figure XI (Part1)

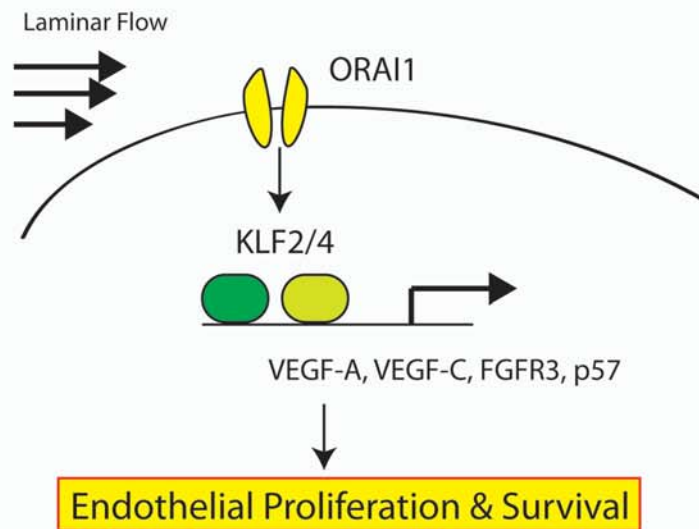
E**F****G**

Online Figure XI (Part2)

A**B**

Online Figure XII

Lymphatic Endothelial Cells



Online Figure XIII